# Analysis of Phase Separation in Compressible Polymer Blends and Block Copolymers

**Junhan Cho**†

*Department of Polymer Science and Engineering, Dankook University, San-8, Hannam-dong, Yongsan-gu, Seoul 140-714, Korea*

*Received April 21, 1999; Revised Manuscript Received December 17, 1999*

ABSTRACT: For the analysis of phase-separation behavior of compressible polymer blends and block copolymer melts, an equation-of-state (EOS) model is combined with the compressible random-phase approximation (RPA) formalism. The EOS model to be employed is obtained from extending an off-lattice model, recently given for interpreting compression response of pure polymers to pressure by Cho and Sanchez (CS), to polymer blends. The free energy for the CS model consists of an ideal free energy of Gaussian chains and a nonideal free energy that represents the excluded volume effects and the attractive interactions in given blend systems. This nonideal free energy yields the RPA interaction fields, with which monomer−monomer correlation functions for polymer blends or block copolymers are calculated to determine the condition of phase separation. It is shown that the theory can predict not only macrophase separation in some polymer blends but also microphase separation in the corresponding block copolymer melts. Especially, microphase separation upon heating, recently observed in several diblock copolymer melts, is shown to be driven by finite compressibility in given copolymer systems. The stability of diblock copolymer melts exhibiting microphase separation upon heating is also discussed in relation to the symmetry of phase diagrams.

## I. Introduction

Incompatible or partially compatible polymer mixtures including polymer blends and block copolymer melts show phase-separation behavior. To understand such behavior is of great importance in the material design viewpoint because morphology developed after phase separation is to a substantial extent responsible for the physical and the mechanical properties of polymeric materials. Polymer blends show the macrophase-separation behavior when they phase separate, which implies that phase separation occurs on a global scale. Meanwhile, block copolymers of two incompatible polymers exhibit a different type of phase separation. Their melts phase separate only on a microscopic scale owing to the connectivity of constituent polymers. The segregated domains have the size of the gyration radius of chains. This phenomenon is called the microphase-separation behavior of block copolymer melts. While macrophase separation in polymer blends can be analyzed with the conventional bulk thermodynamics, the microphase-separation behavior of block copolymer melts is no longer probed with such methods. A relatively simple theoretical tool for the analysis of both the macrophase- and microphase-separation behavior is the random-phase approximation (RPA) introduced to polymer fields by de Gennes.[1,2]

The investigation of phase-separation behavior of polymeric systems is often carried out by using radiation scattering experiments such as small-angle light or neutron scattering. From those scattering experiments, the pair correlations between different monomers, which are also called the liquid structures, are extracted to measure the condition of phase separation. The RPA method provides an approximate scheme to calculate the pair correlations. Since de Gennes first applied RPA to polymer blends,[1,2] this method has been used to calculate pair correlations for diblock[3,4] or multiblock copolymers,[5] the blends of homopolymers and block copolymers,[6−11] and copolymers with more complicated molecular geometry.[5,12] For the calculations just mentioned, the incompressibility constraint has been imposed, and the incompressible Flory−Huggins (FH) theory[13] has been employed for intersegmental interactions.

The phenomena of macrophase separation in nonpolar polymer blends are observed in two ways: polymer blends may phase separate either upon cooling or upon heating. The former case is also called the upper critical solution temperature (UCST) behavior. The latter case is referred to the lower critical solution temperature (LCST) behavior. The UCST behavior is driven by the unfavorable intersegmental interactions in blend systems. This behavior is well described by the incompressible FH theory.[13] The LCST behavior is, however, known to be driven by finite compressibility in blend systems so that the incompressible FH theory fails to describe it. This finding lead to the development of various statistical mechanical equation-of-state models.[14−25]

Most of microphase-separating block copolymer melts had been known to have only the upper critical ordering temperature (UCOT) behavior, which is analogous to the UCST of polymer blends. Block copolymer melts undergo a transition from a disordered state to a microphase-separated state upon cooling. The driving force for this behavior is again the unfavorable intersegmental interactions. As was mentioned before, this behavior is successfully described with the incompressible RPA along with the incompressible FH theory. However, the recent experimental works on the diblock copolymer melts of polystyrene (PS) and lower alkyl polymethacrylates presented by Russell et al.[26−28] found rather the limited phase behavior of block copolymers to be as balanced as that of polymer blends. These block

† A member of Hyperstructured Organic Materials Research Center at Seoul National University, Seoul 151-742, Korea.

10.1021/ma990610n CCC: $19.00 
Published on Web 03/02/2000

copolymer systems studied by Russell et al. showed microphase separation upon heating, which is designated as the lower critical ordering temperature (LCOT) behavior.

The existence of LCOT along with LCST suggests that finite compressibility is responsible for both macrophase and microphase separation at elevated temperatures. This notion has been reflected by the efforts to introduce finite compressibility into RPA by several research groups. Freed and co-workers employed various free volume approaches to study compressibility effects on the correlation functions and other related properties of polymer blends and diblock copolymer melts,[29−32] and later combined the lattice cluster theory[22,23] with RPA.[33−35] The concept of lattice vacancy[19,20] was adopted in the RPA formulations by Yeung et al. to analyze the LCOT behavior of diblock copolymer melts,[36] and by Bidkar and Sanchez to interpret compressibility effects on various scattering properties including interaction parameters of polymer blends.[37] The perturbed hard sphere chain model[24,25] was used by Hino and Prausnitz in an approach similar to that of Yeung et al. to study the phase equilibria of binary polymer blends and diblock copolymer melts.[38]

Meanwhile, Akcasu and co-workers[39,40] suggested a general framework for compressible RPA, based on the linear response theory, that can be readily connected to any specific equation-of-state model for compressible mixtures. The pair correlation functions are described in terms of the pair correlation functions of a reference system and effective interaction fields. The system of noninteracting Gaussian chains is commonly chosen for the reference system because the characteristics of such chains with arbitrary molecular architectures can be treated analytically. It is then through these effective RPA fields that an equation-of-state model for compressible mixtures plays a role in compressible RPA.

The objective of this study is to derive a model-specific compressible RPA. We employ an analytical off-lattice model recently introduced by Cho and Sanchez.[41] The model by Cho and Sanchez (CS model hereafter) can be found from the literature only for pure nonpolar polymers. The CS model is, therefore, to be extended to nonpolar polymer blends. The CS model is based on perturbation theory: the free energy of a chain system is divided into a reference free energy of hard chains and an attractive perturbation energy. The reference free energy of hard chains is subdivided into an ideal free energy of Gaussian chains with no volume exclusion and an excess free energy of hard chains with finite volume exclusion. The former is derived from the direct evaluation of the partition function, whereas the latter is obtained from the integration of the hard chain equation of state from the Baxter−Chiew theory.[42−46] The attractive perturbation energy is obtained from considering locally packed dense polymeric liquids with the random mixing approximation employed to describe the concentration correlations between monomers. The excess free energy of hard chains and the perturbation energy comprise the nonideal free energy of the system. This nonideal free energy is then to yield the effective RPA fields. The derivation of the RPA fields to be presented here is very systematic so that the methodology can be adopted by others with their own choices of models for describing finite compressibility.

In this article, we will mainly focus on the formulation of the effective RPA interaction fields from the CS model with some calculations of the phase diagrams for selected polymer blends and diblock copolymer melts at atmospheric pressure. However, our continuing efforts on this compressible RPA study will be headed toward investigations into pressure effects on the phase boundaries of macrophase- or microphase-segregating systems and the superposition of phase boundary shifts caused by applied pressures. This future plan explains why the CS model is chosen in this study to derive the effective RPA fields. The CS model was developed to aim for pressure effects on the volumetric properties of polymers, especially to interpret the empirically observed temperature−pressure superposition[47−49] in the compression response of pure polymers or homogeneous polymer solutions to pressure.

## II. CS Model for Polymer Blends

In this section, we will present the CS model in detail. The CS model was previously given in the literature for pure polymeric liquids.[41] Its extension to polymer blends is, however, straightforward.

The system of interest is a $m$-component mixture of $N_i$ chains of $n_i$-mers ($i = 1, 2, ..., m$) in a fixed volume $V$. The total number of chains in the system is denoted as $N$ ($=\sum N_i$). We simplify an $n_i$-mer as a linear chain of interacting tangent spheres with $n_i$ sites or monomers spherically interacting with others. The bond potential between the centers of connected spheres is assumed to be infinitely strong, which implies that all the bond lengths are fixed. No restriction in bond angle is imposed. Each monomer is impenetrable; the excluded volume effects are described by the hard sphere potential. All these simplifications then render our model chain an interacting tangent hard sphere chain.

The partition function $Q_N$ of the system can be given by

$$Q_N = \frac{Z_N}{\prod N_i! I_i^{N_i} \Lambda_i^{3n_iN_i}} \tag{1}$$

where the symbol $I_i$ indicates the indistinguishability of an $i$-chain (symmetry number). For homopolymers, $I_i$ should be 2, implying the complete reversion of chains. The symbol $\Lambda_i$ means the thermal de Broigle wavelength of monomers on $i$-chains. In eq 1, $Z_N$ is the configurational partition function of the system

$$Z_N = \int \mathrm{e}^{-\beta V_N} \prod_i \prod_{\gamma_i=1}^{N_i} \mathrm{d}\{\vec{r}_{\gamma_i}\} \tag{2}$$

where $V_N$ is the total potential energy of the system and $\beta = 1/kT$ has its usual meaning. The parentheses in the dummy variable $\{\vec{r}_{\gamma_i}\}$ describes the set of $3n_i$ coordinates for $n_i$ monomers on each $i$-chain.

The total potential $V_N$ is the sum of the intermolecular potential $U_N$ and the intramolecular potential $U_{\mathrm{in}}$. On the simplification of the model chain, the intramolecular potential $U_{\mathrm{in}}$ has only the nonbonded monomer−monomer interaction and the bond potential $U_{\mathrm{in}}^{\mathrm{bond}}$ that holds chains with fixed bond lengths. The total potential upon the pairwise additivity assumption can then be written as

$$V_N = U_N + U_{\mathrm{in}} \approx \sum_{\text{nonbonded}} u_{ij}(\vec{r}) + U_{\mathrm{in}}^{\mathrm{bond}} \tag{3a}$$

where $u_{ij}(r)$ is a given intermer potential between two nonbonded monomers either on the same chain or on two different chains from $i$ and $j$-species, separated by the distance $r$. On the basis of the perturbation theory, the intermer potential $u_{ij}(r)$ is then separated into a reference potential $u_{ij}^{(0)}(r)$ and a proper perturbed potential $u_{ij}^{(1)}(r)$. The system of tangent hard sphere chains is defined as the reference system, which implies that the hard sphere potential is assigned to $u_{ij}^{(0)}(r)$. The sum of all the hard sphere interactions between nonbonded monomers and the bond potential describes the reference total potential $V_N^{(0)}$ for the reference system. The sum of perturbed pair interactions defines the perturbed total potential $V_N^{(1)}$.

$$V_N = V_N^{(0)} + V_N^{(1)} = [\sum_{\text{nonbonded}} u_{ij}^{(0)}(\vec{r}) + U_{\text{in}}^{\text{bond}}] + \sum_{\text{nonbonded}} u_{ij}^{(1)}(\vec{r}) \quad (3b)$$

The reference total potential $V_N^{(0)}$ yields the reference configurational partition function $Z_N^{(0)}$, which gives the reference Helmholtz free energy $A_0$.

$$-\beta A_0 = \ln \frac{Z_N^{(0)}}{\prod N_i! I_i^{N_i} \Lambda_i^{3n_iN_i}} = \ln\left[\frac{1}{\prod N_i! I_i^{N_i} \Lambda_i^{3n_iN_i}} \int e^{-\beta V_N^{(0)}} \prod_i \prod_{\gamma_i=1}^{N_i} d\{\vec{r}_{\gamma_i}\}\right] \quad (4)$$

The direct evaluation of eq 4 even for the simplest system of hard chains is a formidable task because this procedure involves the problem of the separation of intermolecular and intramolecular interactions. However, the reference free energy $A_0$ can be derived in the following way as was presented in our previous communication.[41] The free energy $A_0$ is separated into two terms as

$$A_0 = A_0(\eta \to 0) + [A_0 - A_0(\eta \to 0)] \quad (5)$$

where $\eta$ is the total packing density that implies the fraction of volume occupied by hard sphere chains. The first term in eq 5 represents the free energy of the chain system with zero packing density, which is indeed the system of noninteracting Gaussian chains.[50] The remaining term in eq 5 stands for the hard sphere chain equation of state and is thus simply denoted as $A_0^{\text{EV}}$.

The $A_0^{\text{EV}}$ is directly obtainable, if one knows the reference pressure $P_0$ of the hard chain system

$$\frac{\beta A_0^{\text{EV}}}{N} = \frac{\beta[A_0 - A_0(\eta \to 0)]}{N} = \int_0^\eta \left[\frac{\beta P_0}{\rho} - 1\right]\frac{d\eta}{\eta} \quad (6)$$

where $\rho$ is the total number density of the system. For a reasonably accurate equation for $P_0$ of hard chains, Baxter's compressibility pressure[42,43] for the system of adhesive hard sphere mixtures can be used in conjunction with Chiew's connectivity constraint to build up chains.[44−46] For simplicity, we only consider that all the hard spheres (monomers) in our system of interest have the same diameter $\sigma$. The reference pressure $P_0$ in case of the identical diameter $\sigma$ for all the hard spheres can be found elsewhere as

$$\frac{\beta P_0}{n\rho} = \left[\frac{1}{1-\eta} + \frac{3\eta}{(1-\eta)^2} + \frac{3\eta^2}{(1-\eta)^3}\right] - \left(1 - \frac{1}{n}\right)\frac{1 + \eta/2}{(1-\eta)^2} \quad (7)$$

where $n$ is the representative chain size of the mixture as follows

$$n = \frac{1}{\sum \frac{\phi_i}{n_i}} \quad (8)$$

with the volume fraction $\phi_i$ of $i$-chains defined as

$$\phi_i = \frac{n_i N_i}{\sum n_i N_i} \quad (9)$$

Putting eq 7 into eq 6 yields

$$\frac{\beta A_0^{\text{EV}}}{nN} = \frac{3}{2}\left[\frac{1}{(1-\eta)^2} - \left(1 - \frac{1}{n}\right)\frac{1}{1-\eta}\right] - \frac{1}{n}\left[\ln(1-\eta) + \frac{3}{2}\right] \quad (10)$$

where $nN$ ($=\sum n_i N_i$) is the total number of monomers in the system.

The free energy $A_0(\eta \to 0)$ of Gaussian chains can easily be obtained from the direct manipulation of eq 4 at zero packing density. The reference total potential $V_N^{(0)}(\eta \to 0)$ at zero packing density has only the bond potential $U_{\text{in}}^{\text{bond}}$ to construct the chains with the fixed bond length $\sigma$

$$V_N^{(0)}(\eta \to 0) = U_{\text{in}}^{\text{bond}} = \sum_{i=1}^{m} \sum_{\gamma_i=1}^{N_i} \sum_{j=1}^{n_i} u_{j,j+1}^{\text{bond}}(\vec{r}_{\gamma_i\gamma_i}^{(j,j+1)}) \quad (11)$$

where the vector $\vec{r}_{\gamma_i\gamma_i}^{(j,j+1)}$ connects the centers of two adjacent tangent spheres and $u_{j,j+1}^{\text{bond}}$ denotes the formal notation for the bond potential between them. Equation 11 is indeed the explicit expression of $U_{\text{in}}^{\text{bond}}$. The independence of the Gaussian chains in treating eq 11 yields

$$\int e^{-\beta V_N^{(0)}(\eta \to 0)} \prod_{i=1}^{m} \prod_{\gamma_i=1}^{N_i} d\{\vec{r}_{\gamma_i}\} = \prod_{i=1}^{m} \prod_{\gamma_i=1}^{N_i} \int e^{-\beta \sum_{j=1} u_{j,j+1}^{\text{bond}}(\vec{r}_{\gamma_i\gamma_i}^{(j,j+1)})} d\vec{r}_{\gamma_i}^{(1)} \prod_{l=2}^{n_i} d\vec{r}_{\gamma_i\gamma_i}^{(1,l)} \quad (12)$$

where $\vec{r}_{\gamma_i}^{(1)}$ indicates the position of the first monomer on an $i$-chain and $\vec{r}_{\gamma_i\gamma_i}^{(1l)}$ implies a vector from the first monomer heading for the $l$-th on the same chain. The collection of these vectors describes the spatial position of an $i$-chain. The system volume $V$ that Gaussian chains can visit comes out of each integral in eq 12. The free energy $A_0$ ($\eta \to 0$) can then be written as

$$-\beta A_0(\eta \to 0) = \ln \frac{\prod V^{N_i} z_i^{N_i}}{\prod N_i! I_i^{N_i} \Lambda_i^{3n_iN_i}} \quad (13)$$

where $z_i$ implies the conformational partition function of such Gaussian $i$-chains as

$$z_i = \int e^{-\beta \sum_{j=1}^{\text{bond}} u_{j,j+1}^{\text{bond}}(\vec{r}_{\gamma_i\gamma_i}^{(j,j+1)})} \prod_{l=2}^{n_i} d\vec{r}_{\gamma_i\gamma_i}^{(1,l)} \quad (14)$$

The $z_i$ can be left as an unspecified constant that does not affect any following thermodynamic calculations. Equation 13 can be rewritten by using the definition of $\eta$ ($=\sum n_i N_i \pi\sigma^3/6V$) and $\phi_i$ as

$$\frac{\beta A_0(\eta \to 0)}{nN} = \sum \frac{\phi_i}{n_i} \ln \frac{6\eta\phi_i I_i \Lambda_i^{3n_i}}{\pi n_i \sigma^3 z_i e} \quad (15)$$

where the transcendental number $e$ appears from Stirling's approximation of $N_i!$ in eq 13.

Combining eqs 10 and 15 yields the reference free energy of the hard chain mixture as

$$\frac{\beta A_0}{nN} = \sum \frac{\phi_i}{n_i} \ln \frac{6\eta\phi_i I_i \Lambda_i^{3n_i}}{\pi n_i \sigma^3 z_i e} + \frac{3}{2}\left[\frac{1}{(1-\eta)^2} - \left(1 - \frac{1}{n}\right)\frac{1}{1-\eta}\right] - \frac{1}{n}\left[\ln(1-\eta) + \frac{3}{2}\right] \quad (16)$$

The ensemble average, $\langle V_N^{(1)}\rangle_0$, of the perturbed total potential $V_N^{(1)}$ is given as the sum of all possible perturbed interactions between nonbonded monomers

$$\langle V_N^{(1)}\rangle_0 = \frac{V}{2}\sum_{i,j}(n_i\rho_i)\int u_{ij}^{(1)}(r)[n_j\rho_j g_{ij,0}(r) + \delta_{ij}\omega_{i,0}^{\text{nb}}(r)]4\pi r^2\, dr \quad (17)$$

where $\rho_i = N_i/V$ is the number density of $i$-chains. The function $g_{ij,0}(r)$ is the average intermolecular distribution function between monomers on $i$ and $j$-chains, which counts the adjacent monomers that are not on the same chain. Another function $\omega_{i,0}^{\text{nb}}(r)$ is the average intramolecular distribution function between nonbonded monomers on an $i$-chain, which counts the adjacent nonbonded monomers on-the same chain. The subscript 0 in eq 17 denotes the reference system of hard chains. We should notice that the averaging procedure is performed with the distribution functions for the reference system.

To obtain a tractable and compact expression for $\langle V_N^{(1)}\rangle_0$, we employ a few approximations. The mean field random mixing approximation is applied to the concentration correlations. This approximation excludes any preferred pairs of monomers. The contact probability between nonbonded monomers is estimated from the bulk concentrations. If an arbitrary monomer is selected and the number of its nonbonded nearest neighbors is $h_z$, then the number of its nonbonded nearest neighbors from $j$-chains becomes $\phi_j h_z$ in this mean field estimation.

The local packing of nonbonded nearest-neighbor monomers in dense polymeric liquids is taken into consideration for the monomer density correlations as was given in our previous work on pure polymers.[41] An arbitrarily chosen monomer and its nearest neighbors, which are densely packed, are considered as a building unit of the whole system. It is further assumed that the perturbed pair interactions in this minimal volume unit act on a central monomer at the most probable distance $r_e$ *on average*. The random mixing approximation and the local packing approximation together lend the mathematical representation of the whole procedure in measuring the total $i$, $j$-pair interaction energy as

$$\int u_{ij}^{(1)}(r)[n_j\rho_j g_{ij,0}(r) + \omega_{i,0}^{\text{nb}}(r)\delta_{ij}]4\pi r^2\, dr \approx \phi_j h_z u_{ij}^{(1)}(r_e) \quad (18)$$

In eq 18, we focus on the contribution to the perturbation energy from the nearest neighbors only, which is of our primary concern. Putting eq 18 into eq 17 yields $\langle V_N^{(1)}\rangle_0$ as

$$\langle V_N^{(1)}\rangle_0 = \frac{V}{2}\sum_{i,j} n_i\rho_i\phi_j h_z u_{ij}^{(1)}(r_e) = \frac{nN}{2}\sum_{i,j}\phi_i\phi_j h_z u_{ij}^{(1)}(r_e) \quad (19)$$

This local packing approximation is an improvement over the widely used van der Waals approximation in calculating the perturbation energy. The van der Waals approximation focuses on one selected monomer. All the other nonbonded monomers form an average molecular field that acts on the chosen monomer. The average field in the van der Waals approximation, therefore, results in a uniform background energy. In the local packing approximation, the selected monomer and its nonbonded nearest neighbors are tagged together. All the other monomers outside this minimal volume unit form an average molecular field that affects the local ordering considered here.

One needs to specify a perturbed intermer potential $u_{ij}^{(1)}(r)$ in order to estimate pair interactions in real polymeric systems. The following Mie potential is employed here as $u_{ij}^{(1)}(r)$ as

$$u_{ij}^{(1)}(r) = f_p\epsilon_{ij}\left[\left(\frac{\sigma}{r}\right)^p - \left(\frac{\sigma}{r}\right)^6\right] \quad (20)$$

where $u_{ij}^{(1)}(r)$ acts only at $r > \sigma$. The $\sigma$ is the hard core diameter of monomers as defined previously. The $\epsilon_{ij}$ is the potential depth of the interaction between two monomers on $i$ and $j$-species. We take the exponent $p = 12$ and the prefactor $f_p = 4$, which lend the Lennard-Jones (L-J) potential as one case of the more general Mie potential in eq 20. Other potentials than the L-J potential will not be used in this study. However, the choice of $p$ and $f_p$ may vary from those chosen. The L-J potential is not an exclusive choice for nonpolar polymers.[41]

The intermer potential $u_{ij}^{(1)}(r)$ in eq 20 is then inserted into eq 19:

$$\langle V_N^{(1)}\rangle_0 = \frac{nN}{2}\sum_{i,j}\phi_i\phi_j h_z f_p\epsilon_{ij}\left[\left(\frac{\sigma}{r_e}\right)^p - \left(\frac{\sigma}{r_e}\right)^6\right] \quad (21)$$

The distance parameter $r_e$ in eq 21 is assumed to be related to the average volume $v$ per monomer as

$$v \equiv \frac{V}{nN} \approx \gamma r_e^3 \quad (22)$$

where $\gamma$ is a proper geometric constant. We adopt $\gamma = 1/\sqrt{2}$ from the face-centered-cubic lattice. The $h_z$ is assumed to be constant in dense polymeric liquids. All the volume dependence of the perturbation energy is then concentrated on eq 22. Using the definition of the packing density $\eta$, the average perturbed potential $\langle V_N^{(1)}\rangle_0$ can finally be written as

$$\frac{\langle V_N^{(1)}\rangle_0}{nN} = \frac{1}{2} f_p \sum_{ij} \phi_i \phi_j \bar{\epsilon}_{ij} [(\gamma/C)^{p/3} \eta^{p/3} - (\gamma/C)^2 \eta^2] \quad (23)$$

where $h_z$ has been merged into $\bar{\epsilon}_{ij}$ by defining it as $\bar{\epsilon}_{ij} \equiv h_z \epsilon_{ij}$. The specific value of $h_z$ is, therefore, not important in any of the following calculations. The symbol $C$ is merely $\pi/6$.

The conventional first-order perturbation approximation to the Helmholtz free energy $A$ yields the Gibbs−Bogoliubov upper limit of the free energy as[51]

$$\frac{\beta A}{nN} = \frac{\beta A_0(\eta \to 0)}{nN} + \frac{\beta A_0^{\mathrm{EV}}}{nN} + \frac{\beta \langle V_N^{(1)}\rangle_0}{nN}$$
$$= \sum \frac{\phi_i}{n_i} \ln \frac{6\eta \phi_i I_i \Lambda_i^{3n_i}}{\pi n_i \sigma^3 z_i e} + \frac{3}{2}\left[\frac{1}{(1-\eta)^2} - \left(1 - \frac{1}{n}\right)\frac{1}{1-\eta}\right] - \frac{1}{n}\left[\ln(1-\eta) + \frac{3}{2}\right] + \frac{1}{2} f_p \beta \bar{\epsilon} [(\gamma/C)^{p/3} \eta^{p/3} - (\gamma/C)^2 \eta^2] \quad (24)$$

where $\bar{\epsilon}$ is simply the average interaction parameter for mixtures defined as

$$\bar{\epsilon} = \sum_{ij} \phi_i \phi_j \bar{\epsilon}_{ij} = \sum_i \phi_i \bar{\epsilon}_{ii} - \frac{1}{2} kT \sum_{i,j} \phi_i \phi_j \chi_{ij} \quad (25)$$

In eq 25, $kT\chi_{ij}$ is related to the frequently used exchange energy $\Delta\bar{\epsilon}_{ij}$ given as

$$kT\chi_{ij} \equiv 2\Delta\bar{\epsilon}_{ij} \equiv \bar{\epsilon}_{ii} + \bar{\epsilon}_{jj} - 2\bar{\epsilon}_{ij} \quad (26)$$

The Gibbs free energy $G$ is then given by the Legendre transformation of the Helmholtz energy $A$ in eq 24 with respect to the system volume $V$.

To apply eq 24 to polymer blends, one needs various molecular parameters such as $\bar{\epsilon}_{ii}$, $n_i$, and $\sigma$ for constituent homopolymers and $\bar{\epsilon}_{ij}$ for cross-interaction between dissimilar species. Pure polymer parameters ($\bar{\epsilon}_{ii}$, $n_i$, and $\sigma$) are obtained from fitting the compression data of individual polymers to the following equation of state coming from eq 24

$$P = \frac{kT}{v^*}\left[\frac{3}{2}\frac{(\eta^2 + \eta^3)}{(1-\eta)^3} + \frac{\eta}{n}\frac{(1+\eta/2)}{(1-\eta)^2}\right] + \frac{f_p}{2}\frac{\bar{\epsilon}}{v^*}\left[\frac{p}{3}(\gamma/C)^{p/3}\eta^{p/3+1} - 2(\gamma/C)^2\eta^3\right] \quad (27)$$

where $v^*$ ($=\pi\sigma^3/6$) is the hard core volume of one monomer. Any regression routine can be employed for the data reduction procedure. We assumed the identical $\sigma$ for any monomeric unit in order to simplify the mixture model.[52] Therefore, the regression analysis is performed only to determine $\bar{\epsilon}_{ii}$ and $n_i$ for homopolymers used in this work with $\sigma$ preset to a reasonable value. The $\sigma$ does not always correspond to the chemical repeating unit of a given polymer, but indicates the size of properly renormalized theoretical monomers. The cross-interaction parameter $\bar{\epsilon}_{ij}$ is the true parameter for mixtures. It is widely used to estimate $\bar{\epsilon}_{ij}$ as the geometric mean $(\bar{\epsilon}_{ii}\,\bar{\epsilon}_{jj})^{1/2}$ of self-interaction parameters $\bar{\epsilon}_{ii}$'s.[53] However, the geometric mean rule does not always work in fitting various mixture behavior. This deviation is corrected by adopting $\bar{\epsilon}_{ij} = \xi(\bar{\epsilon}_{ii}\,\bar{\epsilon}_{jj})^{1/2}$ with an adjustable parameter $\xi$.

The free energies for the CS model enable us to determine the stability condition of a given blend system. A stable ($N_i$, $P$, $T$) ensemble of a binary blend system satisfies the following inequality

$$\frac{\partial^2(G/nN)}{\partial\phi_1^2} = \frac{1}{n_1\phi_1} + \frac{1}{n_2\phi_2} - \left\{-f_p\chi u(\eta) + \frac{v\beta_T}{kT}\left[\frac{\partial P}{\partial\phi_1}\right)_{T,V}\right]^2\right\} > 0 \quad (28)$$

where $u(\eta)$ is simply a function of packing density $\eta$ defined as $[(\gamma/C)^{p/3}\eta^{p/3} - (\gamma/C)^2\eta^2]$. It should be noted that $u(\eta)$ is negative in the useful $\eta$ range. The $\partial P/\partial\phi_1$ implies the concentration coefficient of the system pressure and the $\beta_T$ ($\equiv -\partial \ln V/\partial P)_T$) is the isothermal compressibility of the system. These two properties are easily obtained from the proper differentiation of eq 27. The system becomes unstable when the inequality in eq 28 is reversed. The boundary between stability and instability conditions defines the spinodals ($\partial^2(G/nN)/\partial\phi_1^2 = 0$).

The principle merit of the CS model is that the model offers a theoretical interpretation of the empirically observed temperature−pressure ($T-P$) superposition in compression behavior.[47−49] The empirical $T-P$ superposition principle states that compression isotherms are superposed into a universal function of a dimensionless pressure, $\beta_0 P$ or $P/B_0$, where $\beta_0$ and $B_0$ are $\beta_T$ and the bulk modulus $B$ ($=1/\beta_T$) at atmospheric pressure, respectively. In an alternative statement, the shape of the free energy, which is described by the pressure derivatives of $B$ at atmospheric pressure, is temperature insensitive. It was shown in our previous communication that the packing energy, especially its potential exponents in eq 23, is primarily responsible for this behavior.[41] It is then of our interest to seek an analogous statement of $T-P$ superposition in the shifts of spinodals caused by applied pressures in LCST or LCOT systems, where compressibility is the driving force of phase separation.[54] It is a conjecture at the current stage that $\beta_0$ or $B_0$ again plays an important role in superposing spinodals at various applied pressures. This conjecture will be investigated in our future work by using the compressible RPA developed in the next section in conjunction with the CS model.

## III. Compressible RPA and Interaction Fields

The CS model previously presented will now be connected to Akcasu's compressible RPA formalism.[39,40] As was mentioned before, the monomer pair correlation functions are described by the pair correlation functions of the Gaussian chain system and model-specific RPA interaction fields. The interaction fields will be formulated from the CS model by taking the following steps.

To probe a polymer blend microscopically, one needs to consider the local packing density field $\eta_j(\vec{r})$ of monomers on $j$-chains. The system experiences the thermal fluctuation in the packing density as

$$\delta\eta_j(\vec{r}) = \eta_j(\vec{r}) - n_j N_j v^*/V \quad (29)$$

where $n_j N_j v^*/V$ is the bulk average of the packing density of $j$-chains. Instead of considering every possible concentration fluctuation field $\delta\eta_j(\vec{r})$, we will only focus

on its extremum field value, $\langle \delta\eta_j(\vec{r})\rangle$, which is the ensemble average of $\delta\eta_j(\vec{r})$. The fluctuation is characterized by the monomer pair correlation function $S_{ij}(\vec{r})$ defined as

$$S_{ij}(\vec{r} - \vec{r}') = \langle \delta\eta_i(\vec{r})\, \delta\eta_j(\vec{r}')\rangle \tag{30}$$

A hypothetical external potential $U_i(\vec{r})$ ($i = 1, 2, ..., m$) is assumed to perturb the system to have the mean fluctuation $\langle \delta\eta_j(\vec{r})\rangle$. For weak $U_i$'s, the correlation function $S_{ij}(\vec{r})$ can then be identified as the linear response function in the following matrix equation

$$\langle \delta\bar{\eta}(\vec{r})\rangle = -\beta \int \bar{S}(\vec{r} - \vec{r}')\, \bar{U}(\vec{r}')\, \mathrm{d}\vec{r}' \tag{31}$$

where $\langle \delta\bar{\eta}(\vec{r})\rangle$ and $\bar{U}(\vec{r})$ are the column vectors of the corresponding elements. Likewise, $\bar{S}(\vec{r})$ denotes the matrix of $S_{ij}(\vec{r})$'s. In Fourier form, eq 31 can be rewritten as

$$\langle \delta\bar{\eta}(\vec{q})\rangle = -\beta \bar{S}(\vec{q})\, \bar{U}(\vec{q}) \tag{32}$$

where $\vec{q}$ is the scattering vector with $|\vec{q}| = q$. The Fourier transformed correlation function $S_{ij}(\vec{q})$ is also called the static structure factor.

The fundamental step of the compressible RPA is to calculate the mean fluctuation $\langle \delta\bar{\eta}(\vec{q})\rangle$ in the following way. We choose an arbitrary reference system that lacks certain effective pair interactions. The structure factor matrix $\bar{S}(\vec{q})$ in eq 32 is replaced with $\bar{S}^0(\vec{q})$ of the chosen reference system. The external potential is then corrected to properly take the interaction effect on $\langle \delta\bar{\eta}(\vec{q})\rangle$ into account by the matrix $\bar{W}$ as

$$\langle \delta\bar{\eta}(\vec{q})\rangle = -\beta \bar{S}^0(\vec{q})\{\bar{U}(\vec{q}) + \bar{W}\langle \delta\bar{\eta}(\vec{q})\rangle\} \tag{33}$$

where an element $W_{ij}$ of the matrix $\bar{W}$ describes the effective interaction between two nonbonded monomers from $i$ and $j$-species. Therefore, $\bar{W}$ is called the matrix of interaction fields.

Rearranging eq 33 yields

$$\langle \delta\bar{\eta}(\vec{q})\rangle = -\{[\beta \bar{S}^0(\vec{q})]^{-1} + \bar{W}\}^{-1} \bar{U}(\vec{q}) \tag{34}$$

Comparing eq 34 with the original expression in eq 32 for $\langle \delta\bar{\eta}(\vec{q})\rangle$ shows us that

$$[\beta \bar{S}(\vec{q})]^{-1} = [\beta \bar{S}^0(\vec{q})]^{-1} + \bar{W} \tag{35}$$

The best known reference system of noninteracting Gaussian chains is chosen to calculate $\bar{S}^0(\vec{q})$. The matrix $\bar{W}$ needs a theoretical model that has the Gaussian chain system as a limiting case, which is indeed so for the CS model. In the derivation of the CS model, the free energy $A$ is divided into the $A_0(\eta \to 0)$ of Gaussian chains, $A_0^{\mathrm{EV}}$, and $\langle V_N^{(1)}\rangle_0$. We redefine $A_0(\eta \to 0)$ as the reference free energy for the compressible RPA. The remaining terms, $A_0^{\mathrm{EV}}$ and $\langle V_N^{(1)}\rangle_0$, form a nonideal free energy, denoted as $A^{\mathrm{ni}}$, which will eventually give information on $\bar{W}$ later in this section.

To obtain a model-specific $\bar{W}$, we consider the relationship between the structure factor $S_{ij}(0)$ at zero $q$ and the free energy. For a ($\mu_i$, $V$, $T$) ensemble of a polymer blend, where $\mu_i$ is the chemical potential of $i$-chains, $S_{ij}$-(0) describes the global fluctuations in the number of chains in this ensemble.

$$S_{ij}(0) = \frac{n_i n_j v^{*2}}{V}\langle \delta N_i \delta N_j\rangle = \frac{n_i n_j v^{*2}}{V}\left(\frac{\partial \bar{N}_i}{\partial \beta\mu_j}\right)_{V,T,\mu'\mathrm{s}} \tag{36}$$

where $\bar{N}_i$ is the bulk average of the number of $i$-chains and $\delta N_i = N_i - \bar{N}_i$. Using the thermodynamics relations, the matrix inversion of eq 36 gives

$$S_{ij}^{-1}(0) = \frac{V}{n_i n_j v^{*2}}\left(\frac{\partial \beta\mu_i}{\partial \bar{N}_j}\right)_{V,T,\bar{N}'\mathrm{s}} = \frac{V}{n_i n_j v^{*2}}\left(\frac{\partial^2 \beta A}{\partial \bar{N}_i \partial \bar{N}_j}\right)_{V,T,\bar{N}'\mathrm{s}} \tag{37}$$

where the definition of $\mu_i$ is used in the last equality. Equation 37 can be suitably rewritten by using the packing density as

$$S_{ij}^{-1}(0) = \left(\frac{\partial^2(\beta A/nN\tilde{v})}{\partial \eta_i \partial \eta_j}\right)_{V,T,\eta'\mathrm{s}} \frac{1}{v^*} \tag{38}$$

where $\tilde{v}$ is the reduced volume and also the inverse of the total packing density $\eta$. The $\beta A/nN\tilde{v}$ in eq 38 is the dimensionless free energy per monomer diluted by free volume in the system.

At the spinodal points for the ($\mu_i$, $V$, $T$) ensemble, which is suitable for the scattering experiments, the following determinant (Det) vanishes:

$$\mathrm{Det}\left[\left(\frac{\partial^2 \beta A}{\partial \bar{N}_i \partial \bar{N}_j}\right)_{V,T,\bar{N}'\mathrm{s}}\right] = 0 \tag{39}$$

Therefore, $\mathrm{Det}[\bar{S}(0)]^{-1} = 0$ or $\mathrm{Det}[\bar{S}(0)] \to \infty$ can equivalently define the spinodal equation. This condition can be said in scattering experiments that at each spinodal point the scattering power upon radiation diverges at zero scattering angle.

It is easily seen that the inverse Gaussian structure factor at zero $q$ can be obtained from the Gaussian free energy in eq 15, being inserted into eq 38.

$$S_{ij}^0(0)^{-1} = \frac{\partial^2(\beta A_0(\eta \to 0)/nN\tilde{v})}{\partial \eta_i \partial \eta_j}\frac{1}{v^*} = \frac{\delta_{ij}}{n_i \eta \phi_i v^*} \tag{40}$$

Equation 35 then implies that the second-order derivatives of the intensive nonideal free energy $\beta A^{\mathrm{ni}}/nN\tilde{v}$ yield the interaction fields $W_{ij}$'s at zero $q$.

$$\beta W_{ij} = \frac{\partial^2(\beta A^{\mathrm{ni}}/nN\tilde{v})}{\partial \eta_i \partial \eta_j}\frac{1}{v^*} \tag{41a}$$

As $A^{\mathrm{ni}}$ is the sum of $A_0^{\mathrm{EV}}$ in eq 10 and $\langle V_N^{(1)}\rangle_0$ in eq 23, each gives the following contribution to $W_{ij}$

$$\frac{\partial^2(\beta A_0^{\mathrm{EV}}/nN\tilde{v})}{\partial \eta_i \partial \eta_j} \equiv L_{ij}(\eta) = \frac{3}{2}\left[\frac{4}{(1-\eta)^3} + \frac{6\eta}{(1-\eta)^4} - \left(2 - \frac{1}{n_i} - \frac{1}{n_j}\right)\frac{1}{(1-\eta)^2} - \left(\eta - \frac{\eta}{n}\right)\frac{2}{(1-\eta)^3}\right] + \left(\frac{1}{n_i} + \frac{1}{n_j}\right)\frac{1}{1-\eta} + \frac{\eta}{n}\frac{1}{(1-\eta)^2} \tag{41b}$$

and

$$\frac{\partial^2(\beta\langle V_N^{(1)}\rangle_0/nN\tilde{v})}{\partial\eta_i\partial\eta_j} \equiv -\beta\epsilon_{ij}^{\text{app}}(\eta) = \beta\bar{\epsilon}_{ij}f_p\frac{u(\eta)}{\eta} + \beta(\sum_k \eta_k\{\bar{\epsilon}_{ik}+\bar{\epsilon}_{jk}\})f_p\frac{\partial}{\partial\eta}\left(\frac{u(\eta)}{\eta}\right) + \frac{1}{2}\beta(\sum_{kl}\eta_k\eta_l\bar{\epsilon}_{kl})f_p\frac{\partial^2}{\partial\eta^2}\left(\frac{u(\eta)}{\eta}\right) \quad (41c)$$

where $L_{ij}$ and $\epsilon_{ij}^{\text{app}}$ are introduced for notational convenience. The $W_{ij}$ can now be written as

$$\beta W_{ij} = [L_{ij}(\eta) - \beta\epsilon_{ij}^{\text{app}}(\eta)]\frac{1}{v^*} \quad (41d)$$

The minus sign in front of $\epsilon_{ij}^{\text{app}}(\eta)$ in eq 41c is intentionally included, which is, however, a matter of definition.

We have derived the Gaussian structure factors and the RPA interaction fields at zero $q$ from the CS model. The generalization of these functions at an arbitrary $q$ is as follows. The inverse Gaussian structure factor $S_{ij}^0(\vec{q})^{-1}$ at $q$ can be given as[1]

$$S_{ij}^0(\vec{q})^{-1} = \frac{\delta_{ij}}{n_i\eta\phi_i v^*\, g(x_i)} \quad (42)$$

where $\delta_{ij}$ is the Kronecker delta. The $g(x_i)$ is the Debye function of an ideal $i$-chain defined as

$$g(x_i) = \frac{2}{x_i^2}[x_i + e^{-x_i} - 1] \quad (43)$$

where the $x_i$ is the square of the reduced scattering vector given as

$$x_i = q^2R_{G,i}^2 \quad (44)$$

with $R_{G,i}$ denoting the radius of gyration of an ideal $i$-chain.

The interaction matrix $\bar{W}$ at an arbitrary $q$ can be approximated to $\bar{W}$ at zero $q$ given in eq 41. There are some reasons to take this notion. The CS model adopts the mean field approximation in describing the concentration correlations. In addition, the characteristic length associated with the monomer density correlations is small and has the order of magnitude of 1 − 10 Å.[37] Therefore, in the region of $q$, where $1/q$ far exceeds this characteristic length, $\bar{W}$ can be considered constant. The constancy of $\bar{W}$ holds in the small-angle light or neutron scattering, where $1/q > 100$ Å.

There are some features of the structure factors from our compressible RPA that are not seen in the conventional incompressible RPA. In the case of a binary blend of A and B homopolymers, eqs 35, 41, and 42 yield

$$v^*[\bar{S}]^{-1} = \begin{bmatrix} v^*/S_{11}^0 + L_{11} - \beta\epsilon_{11}^{\text{app}} & L_{12} - \beta\epsilon_{12}^{\text{app}} \\ L_{12} - \beta\epsilon_{12}^{\text{app}} & v^*/S_{22}^0 + L_{22} - \beta\epsilon_{22}^{\text{app}} \end{bmatrix} \quad (45)$$

where the subscript 1 indicates A. As can be seen in eq 45, there are the three independent structure factors in the compressible RPA. The first structure factor $S_{11}$ is given from inverting eq 45 as

$$\frac{1}{v^*}S_{11} = \frac{v^*/S_{22}^0 + L_{22} - \beta\epsilon_{22}^{\text{app}}}{(v^*/S_{22}^0 + L_{22} - \beta\epsilon_{22}^{\text{app}})(v^*/S_{11}^0 + L_{11} - \beta\epsilon_{11}^{\text{app}}) - (L_{12} - \beta\epsilon_{12}^{\text{app}})^2} \quad (46)$$

Other two structure factors can be obtained in the same way. The structure factors from the compressible RPA are dependent on every $\epsilon_{ij}^{\text{app}}$ (or $\bar{\epsilon}_{ij}$) and $L_{ij}$. Similar results have also been shown by Freed and co-workers.[29,31,33]

The formal limit of $S_{11}$ at $\eta = 1$ (i.e., no free volume or formal incompressible limit) can be derived from eq 46, even though the total packing density $\eta$ cannot exceed $C/\gamma$ (=0.74) in the CS model.[41] For simplification, let all the chain lengths be large ($n_1 = n_2 \to \infty$, so $L_{ij} = L$ for all $i$ and $j$). As $\eta$ approaches 1, $L$ diverges. A careful manipulation of eq 46 then yields

$$\frac{1}{v^*}S_{11} = \frac{1}{[v^*/S_{11}^0 + v^*/S_{22}^0 - \beta(\epsilon_{11}^{\text{app}} + \epsilon_{22}^{\text{app}} - 2\epsilon_{12}^{\text{app}})]} \quad (47)$$

where all the $\epsilon_{ij}^{\text{app}}$'s in eq 47 are evaluated at $\eta = 1$. Equation 47 is formally identical with that from de Gennes' incompressible RPA.[1,2] One can easily see that $S_{11}$ in eq 47 is the only independent structure factor when $\eta = 1$ because $S_{11} = S_{22} = -S_{12}$. In addition, $S_{11}$ is dependent not on the individual $\epsilon_{ij}^{\text{app}}$'s, but on the exchange energy ($=\epsilon_{ii}^{\text{app}} + \epsilon_{jj}^{\text{app}} - 2\epsilon_{ij}^{\text{app}}$).

## IV. Compressible RPA for Block Copolymers

Our compressible RPA model for polymer blends can easily be extended to block copolymer melts. All that is required is to replace the correlation function $S_{ij}^0(\vec{q})$ of Gaussian blends at an arbitrary scattering vector $q$ with that of Gaussian block copolymer melts. For an A−B diblock copolymer melt as the simplest case, the $S_{ij}^0(\vec{q})$ can be written as[3]

$$S_{11}^0(\vec{q}) = v^*\eta(n_1 + n_2)\, g(\phi_1, x)$$

$$S_{12}^0(\vec{q}) = v^*\eta\frac{(n_1+n_2)}{2}[g(1, x) - g(\phi_1, x) - g(1-\phi_1, x)] \quad (48)$$

$$S_{22}^0(\vec{q}) = v^*\eta(n_1 + n_2)\, g(1-\phi_1, x)$$

where the subscript 1 indicates A and $\phi_1$ is the fraction of A monomers on an A−B diblock copolymer chain. The connectivity of A and B blocks is taken into account in $S_{12}^0(\vec{q})$ in eq 48. The function $g(\phi_1, x)$ is the modified Debye function defined as

$$g(\phi_1, x) = \frac{2}{x^2}[\phi_1 x + e^{-\phi_1 x} - 1] \quad (49)$$

The variable $x$ equals $q^2R_G^2$ as before, where $R_G$ is the gyration radius of a diblock copolymer chain. For other copolymers with arbitrary chain architectures, eq 48 has to be suitably modified. The interaction fields $\bar{W}$ derived for blends can also be used for diblock copolymer melts because A−B diblock copolymer melts are viewed as

locally equivalent to the corresponding blends of A and B homopolymers.

Some significant differences between the compressible RPA and the incompressible RPA for block copolymer melts can be seen in the static structure factors. Equation 45 can be modified for diblock copolymers as

$$v^*[\bar{S}]^{-1} = \begin{bmatrix} v^*S_{22}^0/D + L_{11} - \beta\epsilon_{11}^{app} & -v^*S_{12}^0/D + L_{12} - \beta\epsilon_{12}^{app} \\ -v^*S_{12}^0/D + L_{12} - \beta\epsilon_{12}^{app} & v^*S_{11}^0/D + L_{22} - \beta\epsilon_{22}^{app} \end{bmatrix} \tag{50}$$

where $D$ ($=S_{11}^0\,S_{22}^0 - S_{12}^{0\,2}$) is the determinant of the Gaussian structure factor matrix. In the compressible RPA, the three structure factors in eq 50 are independent. The first structure factor $S_{11}$ is then obtained from inverting eq 50 as

$$\frac{1}{v^*}S_{11} = \frac{\frac{v^*S_{11}^0}{D} + L_{22} - \beta\epsilon_{22}^{app}}{\left(\frac{v^*S_{11}^0}{D} + L_{22} - \beta\epsilon_{22}^{app}\right)\left(\frac{v^*S_{22}^0}{D} + L_{11} - \beta\epsilon_{11}^{app}\right) - \left(-\frac{v^*S_{12}^0}{D} + L_{12} - \beta\epsilon_{12}^{app}\right)^2} \tag{51}$$

The $S_{11}$ is again dependent on every $\epsilon_{ij}^{app}$ and $L_{ij}$ as in the case of polymer blends. We can now formally derive the incompressible limit of $S_{11}$ in eq 51 at $\eta = 1$. Let $L_{ij}$ equal $L$ for all $i$ and $j$ for simplification, which is the case when the chain lengths of A and B blocks are either the same or large enough. Equation 51 can then be manipulated to yield

$$\frac{1}{v^*}S_{11} = \frac{D}{[v^*(S_{11}^0 + S_{22}^0 + 2S_{12}^0) - D\beta(\epsilon_{11}^{app} + \epsilon_{22}^{app} - 2\epsilon_{12}^{app})]} \tag{52}$$

where all the $\epsilon_{ij}^{app}$'s in eq 52 are evaluated at $\eta = 1$ as before. Equation 52 is formally the same as $S_{11}$ from Leibler's incompressible RPA.[3] The exchange energy is again involved in the calculation of $S_{11}$. The other two structure factors at $\eta = 1$ are dependent on $S_{11}$ because $S_{11} = S_{22} = -S_{12}$. The incompressible $S_{11}$ in eq 52 vanishes at zero $q$. This result is caused by vanishing $D$ at zero $q$, which is further attributed to the fact that $S_{ij}^0 \propto \phi_i\phi_j$ at zero $q$.

The compressible RPA yields a strikingly different result about $S_{11}$. It can be shown that eq 51 has its zero $q$ value as

$$\frac{1}{v^*}S_{11}(0) = \frac{S_{11}^0(0)}{S_{11}^0(0)(L_{11} - \beta\epsilon_{11}^{app}) + S_{22}^0(0)(L_{22} - \beta\epsilon_{22}^{app}) + 2S_{12}^0(0)(L_{12} - \beta\epsilon_{12}^{app})} \tag{53}$$

The structure factor $S_{11}(0)$ does not vanish because of the density fluctuations, as Freed and co-workers have shown in their compressible RPA analysis.[29,31] The other two structure factors, which can be obtained from putting appropriate Gaussian structure factors into the numerator in eq 53, do not vanish at zero $q$ either.

**Table 1. Various Molecular Parameters for Homopolymers Used in This Study**

| polymer | $\sigma$ (Å) | $\bar{\epsilon}/k$ (K) | $n\pi\sigma^3/6M$[a] (cm$^3$/g) | average error[b] (cm$^3$/g) |
|---|---|---|---|---|
| PS[c] | 4.039 | 4107.0 | 0.418 57 | 0.000 69 |
| PVME[d] | 3.900 | 3644.8 | 0.429 06 | 0.002 44 |
| PBD[e] | 4.040 | 4065.9 | 0.493 95 | 0.001 58 |
| PCON | 3.996 | 4000.0 | 0.410 00 | |
| PIMA | 3.996 | 3800.0 | 0.420 00 | |

[a] This combined parameter represents the close-packed specific volume of a given polymer with the molecular weight $M$. To obtain the chain size $n$, $M$ should be given. [b] The accuracy of the theoretical equation of state in correlating the volume data of given homopolymers can be enhanced by taking $\sigma$ as one of the molecular parameters to be fitted.[41] [c] Volume data of hydrogenated PS[41,55] are equated to those of deuterated PS to a good approximation.[37,60] [d] Volume data from ref 56. [e] Reference 62.

## V. Compressible RPA Calculations of Spinodals

The compressible RPA is applied to the calculations of the correlation functions and the spinodals of some selected phase-segregating systems. We first choose a well-known LCST system, the blend of deuterated polystyrene (PS) and poly(vinyl methyl ether) (PVME). The three molecular parameters, $\bar{\epsilon}_{ii}$, $n_i$, and $\sigma$, for each homopolymer are tabulated in Table 1. The parameters for PS are obtained from fitting volume data of hydrogenated PS reported by Quach and Simha[41,55] to eq 27. All the three parameters for PS are taken adjustable in performing regression analysis. This procedure results in $\sigma_{PS} = 4.039$ Å as the optimized monomer diameter for PS. The parameters for PVME are obtained from fitting volume data given by Rodgers[56] to eq 27 with only taking $\bar{\epsilon}_{ii}$ and $n_i$ as adjustable. The $\sigma$ for PVME is set to 3.900 Å, which is close to that for PS, prior to parameter estimation. The discrepancy in monomer diameters is resolved in all the following calculations for this blend system by employing the average monomer diameter, $\sigma = (\sigma_i + \sigma_j)/2$, for both polymers. The cross-interaction parameter $\bar{\epsilon}_{ij}$, or alternatively $\xi$, is usually estimated from fitting experimental critical points. The neutron scattering experiments performed on the same blend system by Han et al. show that the blend exhibits the LCST of 425.15 K at $\phi_{PS}^c = 0.19$ when the molecular weights (MW's) of deuterated PS and PVME are 230 000 and 390 000, respectively.[57] The spinodals and LCST are evaluated from eq 28 for different values of $\xi$ to be compared with the experiments. This procedure yields $\xi = 1.002\,64$, which then gives $\Delta\bar{\epsilon}/k = -3.318$; the cross-association is energetically favored. With this $\xi$, the theory predicts the LCST of 425.07 K at $\phi_{PS}^c = 0.19$, which is practically identical to the experimental value. The small difference in monomer diameters in this case helps the present theory to correctly predict $\phi_{PS}^c$.

The correlation functions are now calculated by using eq 35 with the interaction matrix $\bar{W}$ in eq 41. We plot $S_{11}(\vec{q})/v^*$ in Figure 1a, where the subscript 1 denotes PS, as a function of scattering vector $q$ at $\phi_{PS} = 0.19$ and at indicated temperatures. The MW's of PS and PVME in Figure 1 are set to 230 000 and 390 000, respectively, which are the same as those used in the experiments by Han et al. It is typical that $S_{11}(\vec{q})$ has Ornstein−Zernike-type $q$ dependence in small $q$ limit and $1/q^2$ decay in large $q$ limit.[2] Figure 1a reflects such

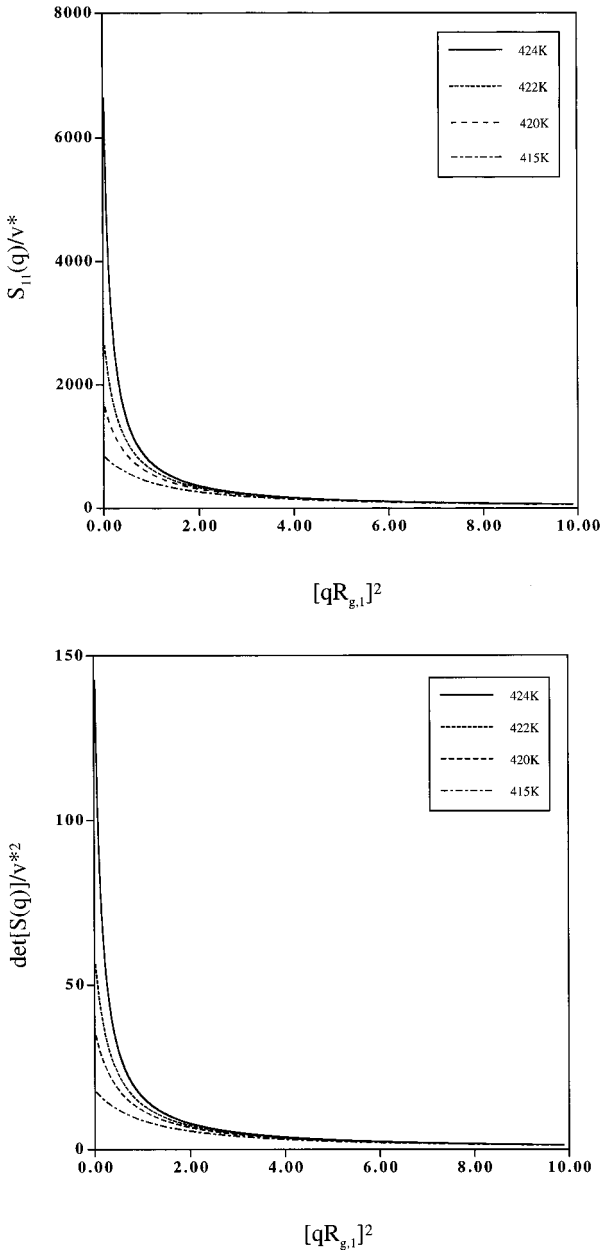


**Figure 1.** $S_{11}(\vec{q})/v^*$ (a, top) and $\mathrm{Det}[\bar{S}(\vec{q})]/v^{*2}$ (b, bottom) plotted as a function of the squared dimensionless scattering vector $[qR_{G,1}]^2$ for the PS(1)/PVME(2) blend at $\phi_{PS} = 0.19$ and at the indicated temperatures. The $R_{G,1}$ indicates the gyration radius of PS chains. The MW's of PS and PVME are 230 000 and 390 000, respectively. The adjustable parameter $\xi$ for $\bar{\epsilon}_{ij}$ is set to 1.002 64. The divergence of $S_{11}(\vec{q})$ and $\mathrm{Det}[\bar{S}(\vec{q})]$ at zero $q$ is caused by heating, which implies the LCST behavior of this system.

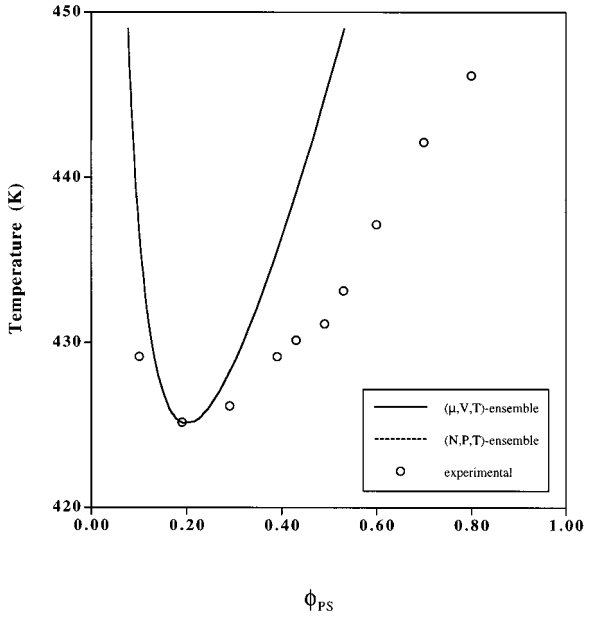


**Figure 2.** Spinodals for the PS/PVME blend in Figure 1 obtained from the compressible RPA for a ($\mu_i$, $V$, $T$) ensemble and from the conventional bulk thermodynamics for a ($N_i$, $P$, $T$) ensemble. The complete coincidence of the spinodals from the two methods is clearly seen. The experimental spinodals (open circles) for the same system measured by Han et al. are also shown for comparison purposes.

asymptotic behavior of $S_{11}(\vec{q})$. As seen in this figure, $S_{11}(\vec{q})$ gradually grows when temperature is increased. One observes the divergence of $S_{11}(\vec{q})$ at zero $q$ and at $T = 425.07$ K. At the same temperature, $\mathrm{Det}[\bar{S}]$ in Figure 1b also diverges at zero $q$, which indicates the macrophase separation in the PS/PVME blend. It is notable that $\mathrm{Det}[\bar{S}]$ vanishes in the incompressible RPA. The temperature of diverging $S_{11}(\vec{q})$ or $\mathrm{Det}[\bar{S}]$ at zero $q$ is the spinodal temperature at the given $\phi_{PS}$. The compressible RPA model predicts macrophase separation upon heating.

The spinodals determined from the method described in Figure 1 for a ($\mu_i$, $V$, $T$) ensemble were recently proved to be equivalent to those from eq 28 for a ($N_i$, $P$, $T$) ensemble.[37,58] This theorem can then be used to verify the correctness of the derived interaction matrix $\bar{W}$ in eq 41. The calculated spinodals of the PS/PVME blend are shown in Figure 2 in the whole range of $\phi_{PS}$. The exact coincidence of the spinodal lines from the two methods is clearly demonstrated in this figure. This result confirms that the interaction field matrix $\bar{W}$ is correct.

For comparison purposes, the experimental spinodals given by Han et al. are also shown in Figure 2. Even though the calculated spinodal curve is narrower than that from the experiments,[59] the asymmetric phase diagram in the PS/PVME blend is correctly predicted. The skewness of the phase diagram for this blend is the well-known evidence of phase separation driven by compressibility difference between PS and PVME.[60] The chain sizes of PS and PVME in Figure 2 are $n_{PS} = 4634$ and $n_{PVME} = 8945$, respectively. As the chain sizes of both homopolymers are large enough, compressibility difference mostly determines the critical composition $\phi^c$; the system becomes rich in a more compressible component at $\phi^c$. Therefore, $\phi^c_{PS} < 0.5$ because PVME is more compressible than PS.

We now turn our attention to the phase behavior of diblock copolymer melts. The system to investigate is the diblock copolymer melt of deuterated PS and PVME, denoted as P(S-b-VME). This system revealed a strong evidence of microphase separation upon heating, yet to be confirmed though, inferred from the recent neutron scattering experiments performed by Hashimoto et al.[61] The calculated $S_{11}(\vec{q})/v^*$ for the P(S-b-VME) melt, where the subscript 1 denotes PS again, is shown in Figure 3a at indicated temperatures. All the molecular parameters for each block and $\xi$ for cross-interaction are the same as those used for the corresponding blend. The MW of P(S-b-VME) is 100 000 0 overall. The volume fraction $\phi_{PS}$ of the PS block is set to 0.293. The shape of $S_{11}(\vec{q})$ in Figure 3a is characteristic of diblock copoly-

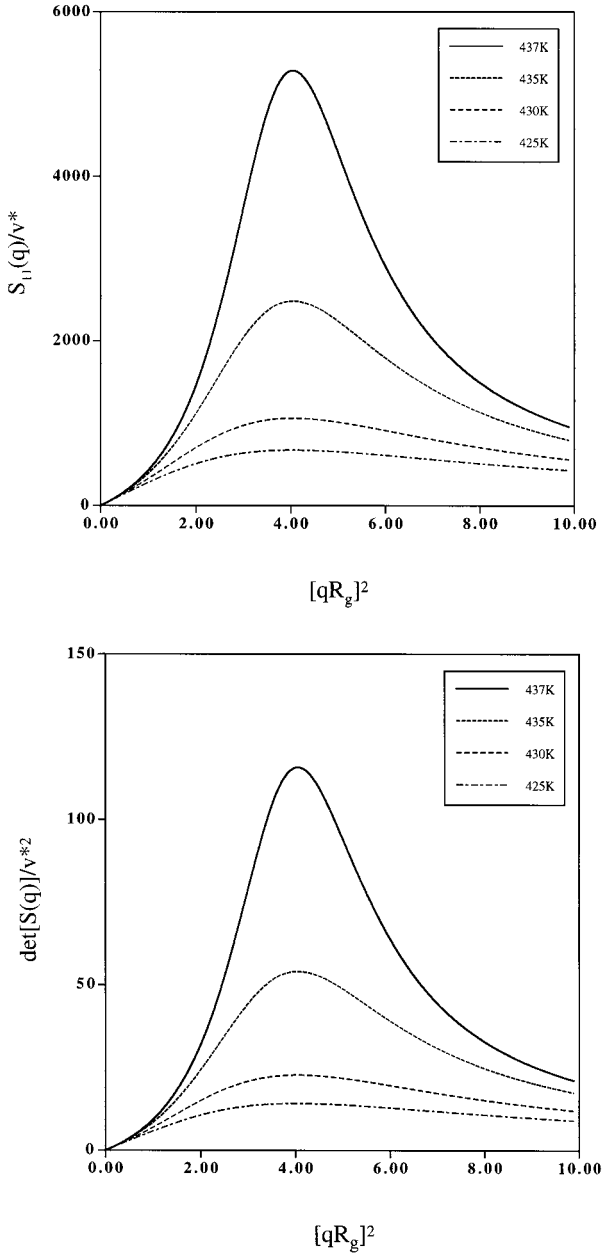


**Figure 3.** $S_{11}(\vec{q})/v^*$ (a, top) and $\mathrm{Det}[\bar{S}(\vec{q})]/v^{*2}$ (b, bottom) plotted as a function of the squared dimensionless scattering vector $[qR_G]^2$ for the P(S-b-VME) melt with MW = 100 000 0 at $\phi_{PS} = 0.293$ and at the indicated temperatures. The subscript 1 in $S_{11}(\vec{q})$ denotes PS as in Figure 1. The $\xi$ is the same as that employed in Figures 1 and 2. The divergence of $S_{11}(\vec{q})$ and $\mathrm{Det}[\bar{S}(\vec{q})]$ at $[qR_G]^2 \sim 4$ is induced by heating, which indicates the LCOT behavior of this system.

mers. The $S_{11}(\vec{q})$ possesses the correlation hole peak[23] with a maximum at $q^2_{max} R^2_G \sim 4$. After passing through a maximum, $S_{11}(\vec{q})$ decays like $1/q^2$. However, $S_{11}(\vec{q})$ from the compressible RPA is distinctly different from its incompressible counterpart: $S_{11}(\vec{q})$ at zero $q$ does not vanish owing to the density fluctuations in the system. The maximum of $S_{11}(\vec{q})$ progressively increases as temperature is elevated. One observes the divergence of this maximum at $T = 438.8$ K, which is the spinodal temperature of the P(S-b-VME) melt at the given composition. Spinodals can be extracted from the divergence of $\mathrm{Det}[\bar{S}]$ as shown in Figure 3b. The $\mathrm{Det}[\bar{S}]$ also possesses a maximum at the same $q_{max}$ eventually to diverge when approaching spinodal temperatures.

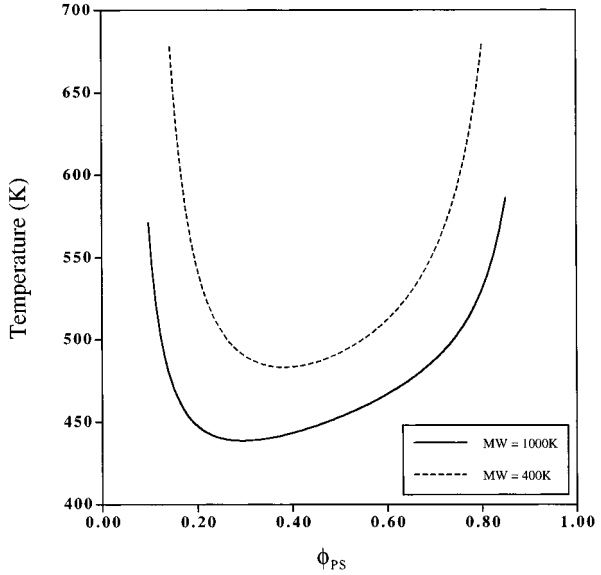


**Figure 4.** Calculated spinodal lines for the P(S-b-VME) melt as a function of $\phi_{PS}$. The thick line represents the copolymer with MW = 100 000 0 and the dotted line that with MW = 400 000. The asymmetric phase diagrams leaning to the PVME-rich side are seen in both cases.

This situation corresponds to the diverging scattering intensity upon radiation at this $q_{max}$, whose inverse gives direct information on the size of microphase-separated domains. Figure 3 then demonstrates that the compressible RPA theory can also predict the suggested microphase separation upon heating in the P(S-b-VME) melt.

Figure 4 shows the spinodals of the P(S-b-VME) melts with the MW's of 100 000 0 and 400 000 in the given region of styrene volume fraction. It is seen in this figure that the P(S-b-VME) melt exhibits LCOT behavior with the lower bound of spinodal temperatures being 438.8 K at $\phi_{PS} = 0.293$ for the former and 488.2 K at $\phi_{PS} = 0.381$ for the latter. The phase diagram for the P(S-b-VME) melt is asymmetric in the same manner as for the PS/PVME blend. Similar results have also been shown by Hino and Prausnitz.[38] It can then be said that compressibility difference is again the driving force of the microphase separation in the P(S-b-VME) melt.

In the experiments done by Hashimoto et al.,[61] the MW of P(S-b-VME) was 23 000 with that of PS block being 9000 ($\phi_{PS} = 0.361$). The scattering intensity from the copolymer, though increased with temperature, did not show a divergence up to 480 K. This result is consistent with our theoretical calculations shown in Figure 4. Because the copolymer with MW = 400 000 is stable up to 488.2 K, the spinodal temperature for the copolymer used in the experiments is predicted to be far beyond 480 K.

The compressible RPA theory can also be used to analyze macrophase or microphase separation upon cooling observed in many systems such as the PS/polybutadiene (PBD) blend and the diblock copolymer of PS and PBD, denoted as P(S-b-BD). We present the predicted phase behavior of the systems just mentioned as illustrations. The $\bar{\epsilon}_{ii}$ and $n_i$ for PBD are obtained from fitting volume data given by Barlow[62] to eq 27 while fixing $\sigma$ to 4.040 Å. All the parameters for PBD are tabulated in Table 1. The parameter $\xi$ for the cross-interaction in the PS/PBD blend is determined by fitting the UCST from the experimental binodals measured by

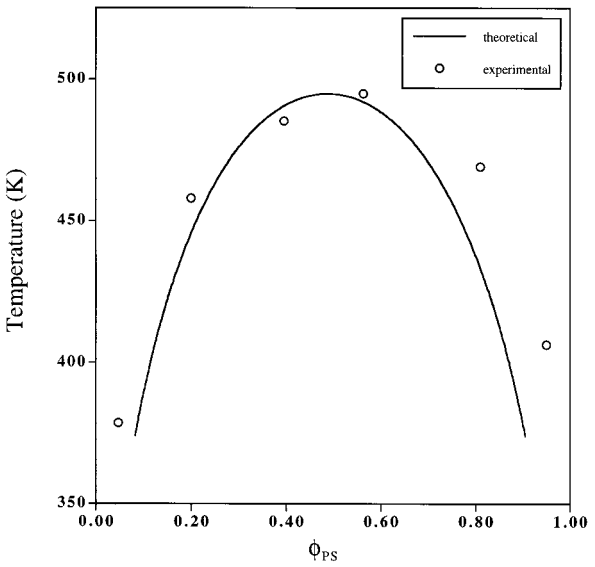


**Figure 5.** Comparison of theoretical and experimental binodals for the PS/PBD blend plotted against $\phi_{PS}$. The MW's of PS and PBD are 3500 and 2660, respectively. The experimental binodals, measured by Zin and Roe, suggest that the system exhibits the UCST of ~495 K. The $\xi$ is determined to be 0.995 65 from fitting the estimated UCST.

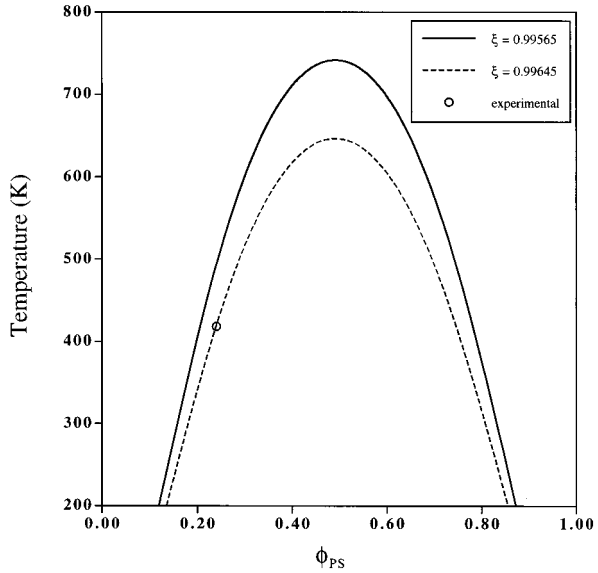


**Figure 6.** The calculated spinodal lines for the P(S-b-BD) melt with MW = 28 000 as a function of $\phi_{PS}$. The thick line represents the predicted spinodals with $\xi$ = 0.995 65, which is obtained for the PS/PBD blend in Figure 5. However, the experimental spinodal point (open circle) for the same copolymer at $\phi_{PS}$ = 0.240, measured by Roe and Zin, is better described by the prediction with $\xi$ = 0.996 45, which is indicated by the dotted line.

Roe and Zin.[63] Comparing the theory with the experiments on this blend with the MW's of 3500 and 2660 for PS and PBD, respectively, yields $\xi = 0.995\ 65$, which then gives $\Delta\bar{\epsilon}/k = 17.828$. Phase separation is driven by this unfavorable energetics. The binodals from the experiments and from the theory are all collected in Figure 5, where the theoretical ones are evaluated from numerically finding coexisting two phases with the identical chemical potentials. As seen in this figure, the agreement between the experiments and the theory is good. By using the same sets of homopolymer parameters and $\xi$, the theoretical spinodals are calculated for the corresponding P(S-b-BD) melt from the divergence of the correlation functions at certain $q_{max}$.

Figure 6 shows such spinodals for the P(S-b-BD) melt with MW = 28 000 overall. It is seen from this figure that the calculated spinodal temperature for the P(S-b-BD) melt with the MW of PS block being 7600 ($\phi_{PS}$ = 0.240) is 495.0 K, which is higher by 76 K than measured from the X-ray scattering experiments performed by Roe and Zin on the same system.[64,65] To fit the scattering experiments on this block copolymer melt, $\xi$ has to be increased to ~0.996 45, which reduces $\Delta\bar{\epsilon}/k$ to 14.558. This discrepancy in the cross-interaction parameters for this oligomeric PS/PBD blend and the P(S-b-BD) melt is also seen in the incompressible RPA analysis presented by Han and co-workers for the same systems.[66] The overestimated spinodal temperature for this copolymer from our compressible RPA is indeed close to that from the incompressible RPA.[66] Hino and Prausnitz in their compressible RPA analysis on the same systems have also shown results similar to ours.[38]

## VI. Stability of Diblock Copolymer Melts with LCOT

It is well-known from Leibler's work on the incompressible RPA that a diblock copolymer melt exhibiting UCOT behavior is more stable than the corresponding symmetric UCST blend.[3,67] The chain size of a diblock copolymer melt needs to be increased to 5.248 times that of each homopolymer in the corresponding symmetric blend in order to have the coincident stability limits or upper bounds of spinodals. Leibler's stability statement is useful in designing diblock copolymers with a controlled miscibility window from the knowledge of the corresponding blends. Leibler's statement from the incompressible RPA can also be regained from our compressible RPA with the CS model. The following calculations of phase diagrams on the PS/PBD system demonstrate this point. The MW's of PS and PBD in their blend are set to 3258 and 2758, respectively. This system is symmetric because the corresponding chain sizes of PS and PBD are $n_{PS}$ = 65.6 and $n_{PBD}$ = 65.5, respectively. These $n_i$'s control the skewness of phase diagrams in UCST blends. The parameter $\xi$ for the cross-interaction is again fixed to 0.995 65, which yields the UCST of 488.2 K at $\phi_{PS}^c$ = 0.502. The P(S-b-BD) melt at $\phi_{PS}$ = 0.5 is then designed to have $n_{PS} + n_{PBD}$ = 344 or MW = 15 785 overall, which is 5.248 times the sizes of the corresponding homopolymers. The calculated phase diagrams for the blend and the diblock copolymer melt are shown in Figure 7. It is seen in this figure that the two upper bounds of spinodals coincide within $\Delta T$ = 1 K and $\Delta\phi_{PS}$ = 0.02. It can be said that Leibler's stability statement is attainable in this UCOT system from our compressible RPA theory. This result implies that the compressible RPA prediction of phase diagrams for UCOT systems at low pressures is little different from the incompressible situation, because compressibility plays a minor role in phase separation upon cooling.

It is of our interest to investigate the applicability of such a stability statement to LCOT systems by using our compressible RPA. Regarding Leibler's stability statement, Yeung et al. suggested that a similar stability condition holds for LCOT systems.[36] We perform theoretical calculations of phase diagrams again on the PS/PVME system. To make the blend symmetric in their sizes, the MW's of PS and PVME are set to 266 200 and

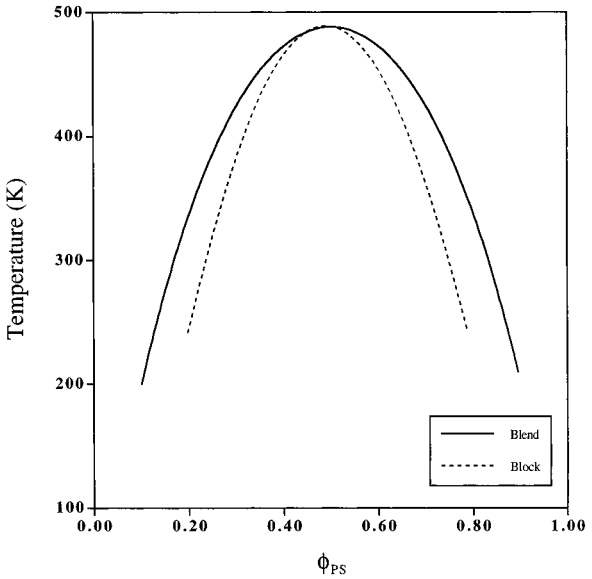


**Figure 7.** Theoretical spinodal lines for the symmetric PS/PBD blend ($n_{PS} = 65.6$ and $n_{PBD} = 65.5$) and the P(S-b-BD) melt as a function of $\phi_{PS}$ with $\xi = 0.995\,65$. The chain size of P(S-b-BD) is set to 5.248 times that of either PS or PBD in the blend. The coincidence of the two upper bounds of spinodals is observed, which indicates Leibler's stability condition of diblock copolymer melts exhibiting UCOT behavior.

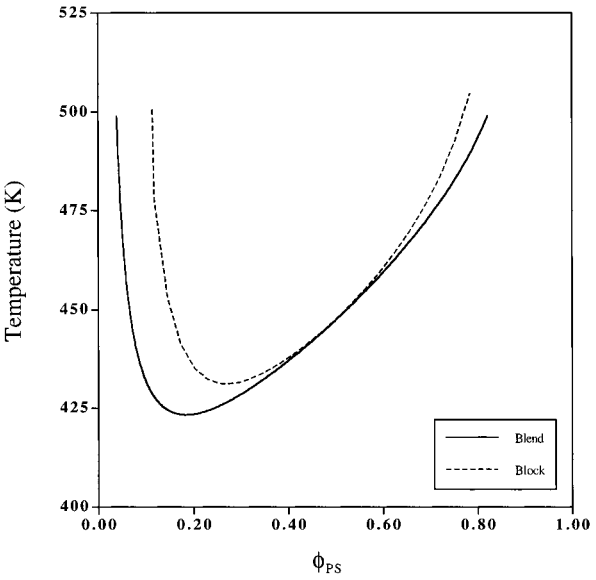


**Figure 8.** Theoretical spinodal lines for the symmetric PS/PVME blend ($n_{PS} = 5364$ and $n_{PVME} = 5362$) and the P(S-b-VME) melt as a function of $\phi_{PS}$ with $\xi = 1.002\,64$. The chain size of P(S-b-VME) is set to 5.248 times that of either PS or PVME in the blend. It is seen that the two lower bounds of spinodals differ from each other by $\Delta T \sim 8$ K and $\Delta\phi \sim 0.08$.

233 800, respectively, which then correspond to $n_{PS} = 5364$ and $n_{PVME} = 5362$, respectively. The P(S-b-VME) melt is designed to have $n_{PS} + n_{PVME} = 28\,145$ or MW = 131 200 0 overall, which is 5.248 times the sizes of homopolymers in the symmetric blend. Figure 8 shows the spinodals for the PS/PVME blend and the P(S-b-VME) melt. It is observed in this figure that Leibler's statement works only qualitatively; the two lower bounds of spinodals differ from each other by $\Delta T \sim 8$ K and $\Delta\phi_{PS} \sim 0.08$. We note that there is strong asymmetry in the phase diagram for this LCOT system, whereas there is always symmetry in those for UCOT systems. This observation suggests that symmetry in

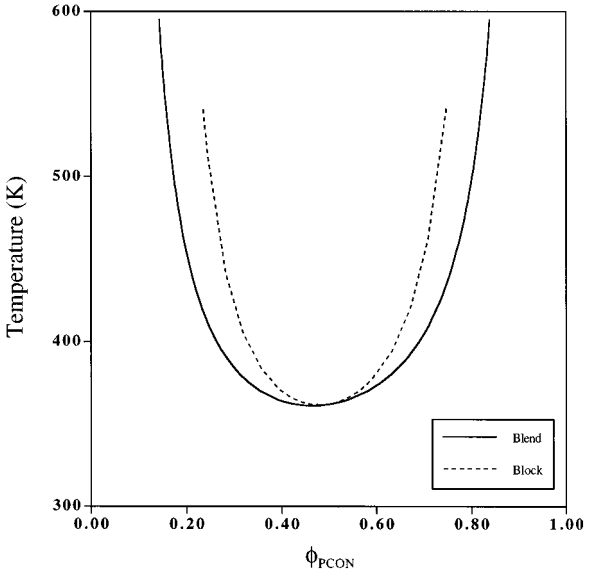


**Figure 9.** Theoretical spinodal lines for the hypothetical PCON/PIMA blend and the corresponding P(CON-b-IMA) melt as a function of $\phi_{PCON}$ with $\xi = 1.0004$. Both PCON and PIMA are of MW = 200 000 with similar chain sizes ($n_{PCON} = 4074$ and $n_{PIMA} = 4174$). The MW of the diblock copolymer is set to 5.248 times those of homopolymers in the blend. The two lower bounds of spinodals are coincident. It should be noted that the phase diagrams for these hypothetical systems are near symmetric.

phase diagrams is deeply related to Leibler's stability statement. We will, therefore, attempt to show the validity of this statement in the case of a LCOT system with a symmetric phase diagram.

The following calculation is performed on a hypothetical LCOT system, denoted as the PCON/PIMA system, that has a symmetric phase diagram when it is phase-separated. The monomer size $\sigma$ of both PCON and PIMA is set to 3.996 Å. All the molecular parameters for the homopolymers are shown in Table 1. The parameter $\xi$ for $\bar{\epsilon}_{ij}$ is set to 1.0004 to place the critical temperature at a suitable position. The MW's of the two polymers in the blend are 200 000 for both. The chain sizes are close to each other: $n_{PCON} = 4074$ and $n_{PIMA} = 4174$. This conceptual blend exhibits the LCST of 361.2 K at $\phi^c_{PCON} = 0.464$, which is practically the symmetric case. It should be kept in mind that all the homopolymer parameters are involved in having proper compressibility difference to set $\phi^c_{PCON}$ to a certain value. It does not suffice to specify only $n_i$'s for setting $\phi^c$ in LCST blends. We now create the hypothetical diblock copolymer of PCON and PIMA, denoted as P(CON-b-IMA), with the MW of 104 960 0 overall, which is again 5.248 times the MW's of the homopolymers in the corresponding blend. The phase diagrams for the blend and the diblock copolymer melt are shown in Figure 9. It is seen that the two lower bounds of spinodals are coincident within $\Delta T = 1$ K and $\Delta\phi_{PCON} = 0.02$. This figure suggests that Leibler's statement for the stability of diblock copolymer melts works for the LCOT systems *with symmetric phase diagrams*.

It has been shown that the applicability of Leiblers stability statement to LCOT systems is limited in a quantitative sense. This statement requires the condition that a given LCOT system possesses a symmetric phase diagram. Nevertheless, Leibler's statement serves as a useful guide in estimating the phase stability of a

given diblock copolymer melt from that of the corresponding homopolymer blend.

## VII. Concluding Remarks

A compressible RPA formalism in connection with an off-lattice equation-of-state model, recently introduced by Cho and Sanchez (denoted as the CS model), is presented here to provide a theoretical tool for analyzing macrophase and microphase separation in compressible polymer blends and block copolymer melts.

The CS model, which was given in the literature only for pure polymers, is extended to a polymer blend system. On the simplification of a polymer chain as interacting tangent hard spheres, interacting with others via the Lennard-Jones (L-J) potential, the free energy for the CS model is divided into a reference free energy of the hard chain blend and a perturbation energy of all L-J interaction pairs. The reference free energy is obtained as the sum of two terms. One is an ideal free energy of the blend of Gaussian chains at zero packing density, which is formulated from the direct evaluation of the partition function. The other is an excess free energy of the hard chain blend at a finite packing density, which is given by the integration of the Baxter−Chiew equation of state for such system. An analytical perturbation energy is formulated from considering the local packing of nearest neighbors in dense polymeric liquids with the random mixing approximation for the concentration correlations between nonbonded monomers. The excess free energy of the hard chain system and the perturbation energy together define the nonideal free energy of the system.

On the basis of a general argument by Akcasu et al. on the compressible RPA, the monomer pair correlation functions of a given system are described by those of the Gaussian chain system and effective RPA interaction fields. The interaction fields for the compressible RPA are formulated from the second-order derivatives of the nonideal free energy for the CS model with respect to the packing densities of constituent homopolymers in the system. The interaction fields are applicable to analyzing not only the phase behavior of polymer blends but also that of the corresponding block copolymer melts.

The compressible RPA presented here approaches in a formal sense the incompressible RPA when no void space is left in the system volume. For binary polymer blends, the classical result of pair correlation functions obtained by de Gennes is reached. For diblock copolymer melts, the pair correlation functions are identical to those obtained by Leibler.

The compressible RPA gives the three independent correlation functions in the case of binary polymer blends or diblock copolymer melts, whereas only one correlation function is independent in the incompressible RPA. The correlation functions in the compressible case are dependent not only on all the self-interaction ($\bar{\epsilon}_{ii}$) and cross-interaction ($\bar{\epsilon}_{ij}$) parameters but also on free volume, whereas only the exchange energy is involved in calculating the correlation functions in the incompressible situation.

The vanishing pair correlation functions at zero $q$ is known to be characteristic of the incompressible RPA for block copolymer melts. It is shown that this property no longer holds in the compressible RPA theory: there is some residual value of correlation functions even at zero $q$ due to the density fluctuations.

At the spinodals of phase-segregating polymer blends or block copolymer melts, the correlation functions $S_{ij}$'s or the determinant Det[$\bar{S}$] from them diverges. The difference between these two types of inhomogeneous systems is the position of $q$ at which the divergence of $S_{ij}$ or Det[$\bar{S}$] happens. Such singularity is observed at zero $q$ for macrophase-separating polymer blends. Microphase-separating block copolymer melts experience this singularity at a certain $q$ that carries information on the microphase-separated domain sizes.

The compressible RPA is applied to the well-known LCST system of the PS/PVME blend. The present theory predicts the system to exhibit a LCST at a PVME-rich composition, which is identical to that measured from the neutron scattering experiments by Han et al. The spinodals for the corresponding P(S-b-VME) melt are then determined to exhibit LCOT behavior, which supports the recent neutron scattering experiments on this copolymer by Hashimoto et al. These results demonstrate that the compressible RPA formulated here proves successful in exhibiting both macrophase- and microphase-separation behavior upon heating, which is unattainable from the incompressible RPA. The macrophase separation driven by finite compressibility in the PS/PVME blend is typified by the skewness of phase diagrams toward the system rich in the more compressible PVME. The phase diagram for the P(S-b-VME) melt also leans to the PVME-rich side, which indicates that the same driving force of phase separation, i.e., compressibility, acts on the copolymer.

The present RPA theory is also applied to the PS/PBD blend and the P(S-b-BD) melt, which exhibit macrophase or microphase separation upon cooling. The phase behavior of these systems predicted by the present theory is shown to be similar to that by the conventional incompressible RPA theory, compared with the experiments performed on the same systems.

In addition, we discuss the stability of a diblock copolymer melt exhibiting LCOT behavior in comparison with the corresponding blend. The well-known result of the stability of diblock copolymer melts is observed in a LCOT system: diblock copolymers are 5.248 times larger in their sizes than the corresponding symmetric polymer blends in order to have the coincident stability limits. A sufficient condition for this statement seems that a LCOT system possesses a symmetric phase diagram by having proper compressibility difference between two constituent homopolymers.

The compressible RPA theory with the CS model for describing finite compressibility is analytical and tractable. The theory can be applied to studies on the phase behavior of various types of polymer mixtures, such as multiblock copolymers, graft or star copolymers, and the blends of homopolymers and block copolymers, etc. The theory may provide a guide to our fundamental query of temperature−pressure superposition in the spinodals of macrophase- or microphase-separating systems via the effective RPA interaction fields formulated from the CS model. This conjecture will lead us to continue our study on the compressible RPA.

**Acknowledgment.** The author is greatly indebted to Professors I. C. Sanchez and W. L. Mattice for having been introduced to the field of polymer physics. The author also gratefully acknowledges Drs. Y. S. Seo and H. J. Choi for their helpful discussions. This work has

been supported by Korea Science and Engineering Foundation through Hyperstructured Organic Materials Research Center.

## References and Notes

(1) de Gennes, P.-G. *J. Phys.* **1970**, *31*, 235.
(2) de Gennes, P.-G. *Scaling Concepts in Polymer Physics*; Cornell University Press: Ithaca, NY, 1979.
(3) Leibler, L. *Macromolecules* **1980**, *13*, 1602.
(4) Fredrickson, G. H.; Leibler, L. *Macromolecules* **1989**, *22*, 1238.
(5) Mayes, A. M.; Olvera de la Cruz, M. *J. Chem. Phys.* **1989**, *91*, 7228.
(6) Leibler, L.; Benoit, H. *Polymer* **1981**, *22*, 195.
(7) Benoit, H.; Wu, W.; Benmouna, M.; Mozer, B.; Bauer, B.; Lapp, A. *Macromolecules* **1985**, *18*, 986.
(8) Mori, K.; Tanaka, H.; Hashimoto, T. *Macromolecules* **1987**, *20*, 381.
(9) Benoit, H.; Benmouna, M.; Wu, W. *Macromolecules* **1990**, *23*, 1511.
(10) Vilgis, T.; Benmouna, M.; Benoit, H. *Macromolecules* **1991**, *24*, 4481.
(11) Kim, J. K.; Kimishima, K.; Hashimoto, T. *Macromolecules* **1993**, *26*, 125.
(12) Olvera de la Cruz, M.; Sanchez, I. C. *Macromolecules* **1986**, *19*, 2501.
(13) Flory, P. J. *Principles of Polymer Chemistry;* Cornell University Press: Ithaca, NY, 1953.
(14) Prigogine, I.; Trappeniers, N.; Mathot, V. *Discuss. Faraday Soc.* **1953**, *15*, 93.
(15) Flory, P. J.; Orwoll, R. A.; Vrij, A. *J. Am. Chem. Soc.* **1964**, *86*, 3515.
(16) Flory, P. J. *J. Am. Chem. Soc.* **1965**, *87*, 1833.
(17) Eichinger, B. E.; Flory, P. J. *Trans. Faraday Soc.* **1968**, *64*, 2035.
(18) Flory, P. J. *Discuss. Faraday Soc.* **1970**, *49*, 7.
(19) Lacombe, R. H.; Sanchez, I. C. *J. Phys. Chem.* **1976**, *80*, 2568.
(20) Sanchez, I. C.; Lacombe, R. H. *Macromolecules* **1978**, *11*, 1145.
(21) Huang, S. H.; Radosz, M. *Ind. Eng. Chem. Res.* **1991**, *30*, 1994.
(22) Dudowicz, J.; Freed, M. S.; Freed, K. F. *Macromolecules* **1991**, *24*, 5096.
(23) Dudowicz, J.; Freed, K. F. *Macromolecules* **1991**, *24*, 5076.
(24) Song, Y.; Lambert, S. M.; Prausnitz, J. M. *Chem. Eng. Sci.* **1994**, *49*, 2765.
(25) Hino, T.; Prausnitz, J. M. *Fluid Phase Equilib.* **1997**, *138*, 105.
(26) Russell, T. P.; Karis, T. E.; Gallot, Y.; Mayes, A. M. *Nature* **1994**, *386*, 729.
(27) Karis, T. E.; Russell, T. P.; Gallot, Y.; Mayes, A. M. *Macromolecules* **1995**, *28*, 1129.
(28) Ruzette, A.-V. G.; Banerjee, P.; Mayes, A. M.; Pollard, M.; Russell, T. P.; Jerome, R.; Slawecki, T.; Hjelm, R.; Thiyagarajan, P. *Macromolecules* **1998**, *31*, 8509.
(29) McMullen, W. E.; Freed, K. F. *Macromolecules* **1990**, *23*, 255.
(30) Dudowicz, J.; Freed, K. F. *Macromolecules* **1990**, *23*, 1519.
(31) Tang, H.; Freed, K. F. *Macromolecules* **1991**, *24*, 958.
(32) Tang, H.; Freed, K. F. *J. Chem. Phys.* **1991**, *94*, 1572.
(33) Dudowicz, J.; Freed, K. F. *J. Chem. Phys.* **1992**, *96*, 9147.
(34) Freed, K. F.; Dudowicz, J. *J. Chem. Phys.* **1992**, *97*, 2105.
(35) Dudowicz, J.; Freed, K. F. *Macromolecules* **1993**, *26*, 213.
(36) Yeung, C.; Desai, R. C.; Shi, A. C.; Noolandi, J. *Phys. Rev. Lett.* **1994**, *72*, 1834.
(37) Bidkar, U. R.; Sanchez, I. C. *Macromolecules* **1995**, *28*, 3963.
(38) Hino, T.; Prausnitz, J. M. *Macromolecules* **1998**, *31*, 2636.
(39) Akcasu, A. Z.; Tombakoglu, M. *Macromolecules* **1990**, *23*, 607.
(40) Akcasu, A. Z.; Klein, R.; Hammouda, B. *Macromolecules* **1993**, *22*, 1238.
(41) Cho, J.; Sanchez, I. C. *Macromolecules* **1998**, *31*, 6650.
(42) Baxter, R. J. *J. Chem. Phys.* **1968**, *49*, 2770.
(43) Barboy, B. *Chem. Phys.* **1975**, *11*, 357.
(44) Chiew, Y. C. *Mol. Phys.* **1990**, *70*, 129.
(45) Malakhov, A. O.; Brun, E. B. *Macromolecules* **1992**, *25*, 6262.
(46) Mitlin, V. S.; Sanchez, I. *C. J. Chem. Phys.* **1993**, *99*, 533.
(47) Sanchez, I. C.; Cho, J.; Chen, W.-J. *J. Phys. Chem.* **1993**, *97*, 6120.
(48) Sanchez, I. C.; Cho, J.; Chen, W.-J. *Macromolecules* **1993**, *26*, 4234.
(49) Sanchez, I. C.; Cho, J. *Polymer* **1995**, *36*, 2929.
(50) Chains should be Gaussian because the system experiences no volume exclusion but keeps the finite number density of chains in a fixed volume. Our perception of chains at $\eta \rightarrow 0$ corresponds to the bead−rod model in polymer dynamics.
(51) Hansen, J.-P.; McDonald, I. R. *Theory of Simple Liquids*; Academic Press: London, 1986.
(52) This condition can be fused by taking the variation of hard sphere diameters for different polymers into account. The free energy in eq 24 should be generalized in accord with varying $\sigma$. This procedure results in a more mathematically involved free energy. However, the assumption of identical $\sigma$ in this study is acceptable because the optimized $\sigma$'s for commonly used polymers are quite uniform, as was shown in our previous work.[41]
(53) Prausnitz, J. M.; Lichtenthaler, R. N.; Gomez de Azevedo, E. *Molecular Thermodynamics of Fluid-Phase Equilibria*, 2nd ed.; Prentice-Hall, Inc.: Englewood Cliffs, NJ, 1986.
(54) A discussion related to this rather unexplored topic was recently given by Rabeony et al. in their empirical approach of treating the interaction strength as a sole function of density. Their approach works well for UCST systems apart from critical points but does not for LCST systems. See: Rabeony, M.; Lohse, D. J.; Garner, R. T.; Han, S. J.; Graessley, W. W.; Migler, K. B. *Macromolecules* **1998**, *31*, 6511.
(55) Quach, A.; Simha, R. *J. Appl. Phys.* **1971**, *42*, 4592.
(56) Rodgers, P. A. *J. Appl. Polym. Sci.* **1993**, *48*, 1061.
(57) Han, C. C.; Bauer, B. J.; Clark, J. C.; Muroga, Y.; Matsushita, Y.; Okada, M.; Tran-cong, Q.; Chang, T.; Sanchez, I. C. *Polymer* **1988**, *29*, 2002.
(58) Higgins, J. S.; Benoit, H. C. *Polymers and Neutron Scattering*; Oxford University Press: Oxford, U.K., 1994.
(59) The narrow spinodal curve for the PS/PVME blend may be broadened by the inclusion of specific interaction character.[60]
(60) Sanchez, I. C.; Balazs, A. C. *Macromolecules* **1989**, *22*, 2325.
(61) Prior to Hashimoto et al.'s experiments, Freed et al. made a prediction by using the RPA with the lattice cluster theory that the P(S-b-VME) melt of MW = 23 000 possesses immiscibility-loop-type microphase separation.[35] Experimental results, however, denied such prediction. The analysis of scattering intensity for the P(S-b-VME) melt of the same MW ($\phi_{PS} = 0.361$) revealed LCOT behavior only. Even though no microphase separation was observed up to 480 K, the scattering intensity increased with temperature. See: Hashimoto, T.; Hasegawa, H.; Hashimoto, T.; Katayama, H.; Kamogaito, M.; Sawamoto, M.; Imai, M. *Macromolecules* **1997**, *30*, 6819.
(62) Barlow, J. W. *Polym. Eng. Sci.* **1978**, *18*, 238.
(63) Roe, R. J.; Zin, W. C. *Macromolecules* **1980**, *13*, 1221.
(64) Zin, W. C.; Roe, R. J. *Macromolecules* **1984**, *17*, 183.
(65) Roe, R. J.; Zin, W. C. *Macromolecules* **1984**, *17*, 189.
(66) Han, C. D.; Kim, J.; Kim, J. K. *Macromolecules* **1989**, *22*, 383.
(67) Fredrickson, G. H.; Helfand, E. *J. Chem. Phys.* **1987**, *87*, 697.

MA990610N